Chemical Engineering Communications
Publication details, including instructions for authors and subscription information:
http://www.informaworld.com/smpp/title~content=t713454788

COMPUTER-AIDED ESTIMATION OF ACETONE, METHYL ACETATE, AND CHLOROFORM DIFFUSION COEFFICIENTS IN POLY(VINYL ACETATE)

G. D. Verros [a]; S. Papahristou [b]; J. Prinos [b]; N. A. Malamataris [c]
[a] Department of Informatics and Computer Technology, Technological Educational Institute (T.E.I.) of Lamia, Lamia, Greece.
[b] Department of Chemical Engineering, Aristotle University of Thessaloniki, Thessaloniki, Greece.
[c] Department of Mechanical and Industrial Engineering, University of Thessaly, Volos, Greece.

To cite this Article: Verros, G. D., Papahristou, S., Prinos, J. and Malamataris, N. A. , 'COMPUTER-AIDED ESTIMATION OF ACETONE, METHYL ACETATE, AND CHLOROFORM DIFFUSION COEFFICIENTS IN POLY(VINYL ACETATE)', Chemical Engineering Communications, 190:3, 334 - 359
To link to this article: DOI: 10.1080/00986440302134
URL: http://dx.doi.org/10.1080/00986440302134

Chem. Eng. Comm., 190: 334–359, 2003

0098-6445/03 $12.00 + .00
DOI: 10.1080/00986440390179262

Taylor & Francis
Taylor & Francis Group

COMPUTER-AIDED ESTIMATION OF ACETONE, METHYL ACETATE, AND CHLOROFORM DIFFUSION COEFFICIENTS IN POLY(VINYL ACETATE)

G. D. VERROS

Department of Informatics and Computer Technology, Technological Educational Institute (T.E.I.) of Lamia, Lamia, Greece

S. PAPAHRISTOU
J. PRINOS

Department of Chemical Engineering, Aristotle University of Thessaloniki, Thessaloniki, Greece

N. A. MALAMATARIS

Department of Mechanical and Industrial Engineering, University of Thessaly, Volos, Greece

The diffusion coefficients of acetone, methyl acetate, and chloroform in amorphous poly(vinyl acetate) are estimated using the solvent evaporation method. The evaporation process from polymer solutions, cast in the form of thin films, is studied as a numerical experiment. The process is modeled as a coupled heat and mass transfer problem with a moving boundary. Lattice fluid (LF) thermodynamics is used to describe polymer-solvent system volumetric properties and to derive appropriate expressions for solvents' chemical potentials. The resulting nonlinear system of governing equations is solved with the Galerkin finite element method. The estimated diffusion coefficients are in satisfactory agreement with reported data.

Address correspondence to G. D. Verros, P.O. Box 454, Plagiari, GR-57500 Epanomi, Greece. E-mail: verros@vergina.eng.auth.gr

Keywords: Diffusion coefficients; Poly(vinyl acetate); Solvent evaporation; Moving boundary; Finite element method

INTRODUCTION

The binary diffusion coefficient in solvent-polymer systems is of major importance for a number of industrial processes, including membrane, foam, and coating formation, devolatilization, mixing of additives and plasticizers, and effectiveness of polymerization reactors at high conversion. In addition, the diffusion of small molecules in a polymer matrix is essential for miscellaneous polymer products such as controlled drug delivery systems, barrier materials, and membranes for separation (Zielinski and Duda, 1996).

The industrial importance of diffusion coefficients in polymer systems has led to extensive work in their measurement and estimation. Measurement techniques include sorption and desorption, radiotracer methods, chromatography, and nuclear magnetic resonance (NMR) experiments as reviewed by Crank and Park (1968), Tyrrell and Harris (1984), and Cussler (1984). Predictive models based on the free volume concepts may be used for the estimation of polymer-solvent diffusion coefficients, as developed by Ju et al. (1981a), Zielinski and Duda (1992), and Vrentas et al. (1996).

The experimental complexities in the measurement of diffusion coefficients and the need for increased accuracy in their estimation was the starting point for the development of the solvent evaporation method. This method combines simple laboratory experiments with advanced modeling in order to get accurate estimates of the diffusion coefficients. In particular, the laboratory experiments consist of gravimetric measurement of the solvent evaporation rate from appropriate cast polymer-solvent films. The measured solvent evaporation rate is compared with model predictions in order to estimate the unknown parameters of diffusion coefficient correlation based on free volume theory.

This idea was proposed by Ataka and Sasaki (1982). However, the implementation of powerful numerical methods such as Galerkin finite elements allowed its realization by studying the solvent evaporation process in the general framework of computational transport phenomena. Price et al. (1997) were the first who got estimates of the diffusion coefficients by fitting drying rate in order to optimize the performance of industrial dryers. Recently, Verros and Malamataris (1999) estimated the binary and the self-diffusion coefficient of an acetone-cellulose acetate system by using established gravimetric measurements of the acetone evaporation rate. The evaporation process was studied as a one-dimensional numerical experiment utilizing the Galerkin finite element method. The numerical technique provides simultaneous solution of the model equations and

yields, by comparison with gravimetric data, the diffusion coefficients of acetone in cellulose acetate over a wide range of temperature and composition. The estimated diffusion coefficients based on free volume theory were in satisfactory agreement with experimental data of Park (1961), Anderson and Ullman (1973), Reuvers and Smolders (1987), and Sanopoulou et al. (1995).

In the present work, the solvent evaporation method is applied to estimate the diffusion coefficients of three liquid solvents, namely, acetone, methyl acetate, and chloroform in poly(vinyl acetate) (PVAC). Despite their importance, little is known about these diffusion coefficients. Kokes et al. (1952) and Ju et al. (1981b) performed sorption experiments to measure binary diffusion coefficients of acetone in PVAC and chloroform in PVAC, respectively. Arnould and Laurence (1992) utilized capillary column inverse gas chromatography to measure the gaseous acetone and methyl acetate diffusion coefficient in PVAC at the limit of pure polymer. However, diffusion of these solvents over a wide range of temperature and concentration has not been studied yet, due to the complexity of experimental methods and modeling techniques. Lattice fluid thermodynamics is used for the first time in this area as it is simple and accurate in describing polymer-solvent interactions as shown by Sanchez and Lacombe (1976a, 1976b), and Panayiotou and Sanchez (1991).

In the next section, a brief description of the experimental part is given and the experimental procedures for preparing solvent-polymer thin films and measuring evaporation rate are described. In the modeling section, the governing equations of the solvent evaporation process are given along with the appropriate initial and boundary conditions. Lattice fluid thermodynamics is introduced in the section on model parameters to describe polymer-solvent interactions. Finally, the finite element formulation is given, results are presented, and conclusions are drawn.

EXPERIMENTAL PART

The aim of this work is to determine the diffusion coefficients of various solvents in amorphous PVAC by comparing the measured evaporation rate with model predictions. The evaporation rate from PVAC solutions cast in the form of thin films was measured gravimetrically, and for this purpose an experimental procedure has been designed, as shown in Figure 1.

The PVAC used was purchased from BDH Chemicals Ltd. (weight-average molecular weight 51,000). The prepared solutions were cast in thicknesses in the range of $180-240\,\mu m$ on clean glass slides ($1 \pm 0.01\,mm \times 70\,mm \times 50\,mm$) with the aid of a "doctor's knife." To measure the solvent evaporation rate gravimetrically, the cast liquid films

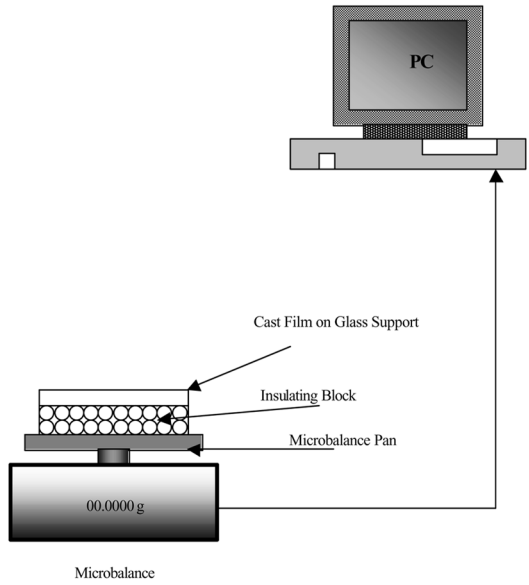

Figure 1. Schematic representation of the experimental setup for solvent evaporation measurement.

(after their preparation) were transferred to a microbalance (accuracy 10^{-4} gr), which was connected to a personal computer for data acquisition (three measurements per second). To prevent heat exchange between the glass slides and the microbalance pan, the glass slides were placed on an insulating block resting upon the microbalance pan (Figure 1). The microbalance was exposed to the ambient air, so that accumulation of solvent vapor in the vicinity of the equipment was avoided and zero solvent concentration in the bulk of gas phase was ensured.

It was found convenient to express the measured evaporation rate in terms of instantaneous solvent/polymer mass ratio because, in this way, the experimental results are presented uniformly. To determine polymer mass, the films were dried for several hours in an oven at 80°C after the evaporation rate measurement, until a constant weight was obtained.

MODELING OF SOLVENT EVAPORATION PROCESS

Governing Equations and Boundary Conditions

The system consists of a liquid layer resting upon an impermeable solid support exposed to a gas phase of temperature T_0, as shown in Figure 1. The liquid layer is the PVAC solution and has an initial thickness L_0.The

support is a flat, horizontal glass plate with constant thickness L_{sup}, allowing heat exchange with the polymer solution. Prior to time zero, the polymer solution has a constant initial solvent concentration everywhere in its mass and the whole system is at initial temperature T_0. At time t = 0, a liquid-gas interface is suddenly created by exposing the polymer solution to the gas phase. The solvent begins to evaporate, resulting in a downward motion of the liquid-gas interface. As the solvent at the surface evaporates, the gas-liquid interface is cooled. From an engineering point of view, this is a coupled heat and mass transfer process with a moving boundary.

Assuming one-dimensional Fickian diffusion, which is valid as it was shown by numerous workers in the area (Shojaie et al., 1992; Vrentas and Vrentas, 1994; Cairncross et al., 1995; Guerrier et al., 1998; Alsoy and Duda, 1999; Verros and Malamataris, 2001a), the governing equations are:

$$\frac{\partial \rho_1}{\partial t} = \frac{\partial}{\partial z}\left(D\frac{\partial \rho_1}{\partial z}\right) \qquad 0 < z < L(t) \tag{1}$$

$$\rho_s C_p \frac{\partial T}{\partial t} = \frac{\partial}{\partial z}\left(k\frac{\partial T}{\partial z}\right) \qquad 0 < z < L(t) \tag{2}$$

$$\frac{\partial T_{\text{sup}}}{\partial t} = \alpha_{\text{sup}}\frac{\partial^2 T_{\text{sup}}}{\partial z^2} \qquad \alpha_{\text{sup}} = k_{\text{sup}}/\rho_{\text{sup}}C_{\text{psup}} \qquad -L_{\text{sup}} < z < 0 \tag{3}$$

The appropriate initial and boundary for the above equations are:

Initial and Boundary Conditions for the Diffusion Equation.

$$\rho_1 = \rho_{10} \qquad t = 0 \tag{4}$$

$$D\partial\rho_1/\partial z = -k_G P(x_s - x_g) \qquad z = L(t) \tag{5}$$

$$\partial\rho_1/\partial z = 0 \qquad z = 0 \tag{6}$$

Equation (5) is the mass balance at the moving interface and Equation (6) specifies zero mass flux at the glass plate.

Initial and Boundary Conditions for the Energy Equations.

$$T = T_{sup} = T_0 \qquad t = 0 \tag{7}$$

$$k\,\partial \mathrm{T}/\partial \mathrm{z} = h(T_g - T_s) + \varepsilon\sigma(T_\infty^4 - T_s^4) - (\Delta H)k_G P(x_s - x_g) \quad z = L(t) \tag{8}$$

$$k_{sup}\ \partial T_{\mathrm{sup}}/\partial z = k\partial T/\partial z \qquad z = 0 \tag{9}$$

$$\partial T_{\mathrm{sup}}/\partial z = 0 \qquad z = -\mathrm{L}_{\mathrm{sub}} \tag{10}$$

Equation (8) is the energy balance at the moving interface, equating the heat conduction to the polymer solution with free convection heat transfer, radiant heat transfer from the ambient air, and latent heat loss due to solvent evaporation. Equation (9) implies continuity of temperature and heat flux at the glass plate-polymer solution interface, while Equation (10) implies perfect insulation of the glass support lower surface.

Conservation of polymer mass gives the following equation for the instantaneous liquid layer thickness, $L(t)$, defining the position of the moving boundary (Vrentas and Vrentas, 1994; Verros and Malamataris, 2001b):

$$\rho_2 \mathrm{dL}/\mathrm{dt} = (DV_1/V_2)(\partial\rho_1/\partial z\ |_{\mathrm{z=L(t)}}) \tag{11}$$

where ρ_2 represents PVAC mass concentration and V_1 and V_2 are the partial specific volumes of the solvent and PVAC, respectively.

To facilitate numerical solution of the problem, the above equations are rendered dimensionless. After dedimensionalizing mass concentration ρ, temperature T, and thickness of the solution L with initial solvent concentration ω_{10}, and initial temperature of the process T_0 and initial thickness of the solution L_0, the dimensionless equations defining the evaporation model become:

Diffusion and Energy Equations.

$$\mathrm{C}_1\frac{\partial\omega_1}{\partial\tau} = \frac{\partial}{\partial\eta}\left(\mathrm{C}_1\mathrm{C}_2\frac{\partial\omega_1}{\partial\eta}\right); \quad C_1 = \left(\rho_s + \omega_1\frac{\partial\rho_s}{\partial\omega_1}\right); \quad C_2 = D/D_0$$
$$0 < \eta < s \tag{12}$$

$$C_3\frac{\partial\Theta}{\partial\tau} = \frac{\partial}{\partial\eta}\left(C_4\frac{\partial\Theta}{\partial\eta}\right); \quad C_3 = \rho C_p/\rho_0 C_{\mathrm{p0}}; \quad C_4 = k/D_0\rho_0 C_{\mathrm{p0}}$$
$$0 < \eta < s \tag{13}$$

$$\frac{\partial\Theta_{\mathrm{sup}}}{\partial\tau} = C_5\frac{\partial^2\Theta_{\mathrm{sup}}}{\partial\eta^2}; \quad C_5 = \alpha_{sup}/D_0; \quad -L_{sup}/L_0 < \eta < 0 \tag{14}$$

Initial and Boundary Conditions for the Diffusion Equation.

$$\omega_1 = \omega_{10} \qquad \tau = 0 \tag{15}$$

$$C_2\partial(\rho_s\omega_1)/\partial_\eta = C_2C_1\partial\omega_1/\partial\eta = C_6(x_s - x_g);$$
$$C_6 = -L_0K_GP/D_0 \qquad \eta = s \tag{16}$$

$$\partial\omega_1/\partial\eta = 0 \qquad \eta = 0 \tag{17}$$

Initial and Boundary Conditions for the Energy Equations.

$$\Theta = \Theta_{sup} = 1 \qquad \tau = 0 \tag{18}$$

$$C_4\partial\Theta/\partial\eta = \mathrm{C_7(\Theta - 1) + C_8(1 - \Theta_s^4) - C_9(x_S - x_g);}\quad \mathrm{C_7 = L_0h/}D_0\rho_0C_{\mathrm{p0}}$$
$$C_8 = L_0\varepsilon\sigma T_0^3/D_0\rho_0C_{p0}; \quad C_9 = (\Delta H)k_GPL_0/(\mathrm{T_0}D_0\rho_0C_{\mathrm{p0}}) \quad \eta = s \tag{19}$$

$$\partial\Theta_{\mathrm{sup}}/\partial\eta = C_{10}\partial\Theta/\partial\eta; \quad \mathrm{C_{10} = k/k_{sup}} \qquad \eta = 0 \tag{20}$$

$$\partial\Theta_{\mathrm{sup}}/\partial\eta = 0 \qquad \eta = -\mathrm{L_{sup}/L_0} \tag{21}$$

Moving Boundary Equation. By substituting Equation (5) in Equation (11) and dedimensionalizing we obtain:

$$\rho_s(1 - \omega_1)\mathrm{ds/d}\tau = C_6(x_s - x_g)V_1/V_2 \tag{22}$$

where $\omega_1 = \rho_1/\rho_{\mathrm{s}}$ is solvent weight fraction, ρ_{s} is polymer solution density, $\eta = z/L_0$ is dimensionless space coordinate, $\tau = D_0t/L_0^2$ is dimensionless time, $\Theta = T/T_0$ is dimensionless temperature, and $s = L(t)/L_0$ is dimensionless position of the moving boundary.

Model Parameters

Thermophysical Properties of the Polymer Solution and the Glass Substrate. The polymer solution density and the solvent chemical potential were calculated using the lattice fluid theory (Sanchez and Lacombe, 1976a, 1976b). According to this theory, reduced density $\tilde{\rho}$ is given as a function of reduced pressure $\tilde{\mathrm{P}}$ and reduced temperature $\tilde{T}$ by the following equation of state:

$$\tilde{\rho}^2 + \tilde{\mathrm{P}} + \tilde{\mathrm{T}}\left[\ln(1 - \tilde{\rho}) + \left(1 - \frac{1}{\mathrm{r}}\right)\tilde{\rho}\right] = 0 \tag{23}$$

where $\tilde{T} \equiv T/T_m^* \equiv RT/\varepsilon_m^*$, $\tilde{P} \equiv P/P_m^* \equiv Pv_m^*/\varepsilon_m^*$, and $\tilde{\rho} \equiv \rho_s/\rho_m^*$. Parameters, ε_m^*, v_m^*, and ρ_m^*, for a binary solution are given by the following mixing rules:

$$\varepsilon_m^* = \sum_{i=1}^{2}\sum_{i=1}^{2} \varphi_i\varphi_j\varepsilon_{ij}; \quad \varepsilon_{12} = \zeta\sqrt{\varepsilon_{11}\varepsilon_{22}}; \quad \varepsilon_{ii} = RT_i^* \quad i = 1,2 \tag{24}$$

$$v_m^* = \sum_{i=1}^{2} \varphi_i v_i^*; \quad v_i^* = \varepsilon_{ii}/P_i^* \quad i = 1,2 \tag{25}$$

$$\frac{1}{\rho_m^*} = \sum_{i=1}^{2} \frac{\omega_i}{\rho_i^*} \tag{26}$$

The segment fraction φ_l is defined by

$$\varphi_i = x_i r_i/r; \quad \mathrm{r} = \sum_{i=1}^{2} x_i r_i; \quad r_i = MP_i^*/\rho_i^* RT_i^* \quad i = 1,2 \tag{27}$$

where ζ is a dimensionless binary parameter expected to have values close to unity, $\mathrm{x_i}$ is the mole fraction of the ith compound, M is molecular weight, and T_i^*, P_i^*, and ρ_i^* are characteristic constants for a compound. Equations (23)–(27) are solved simultaneously by an iterative procedure. In the above equations the final unknown parameters are quantities T_i^*, P_i^*, ρ_i^*, and ζ (see Equations (24)–(27)). The T_i^*, P_i^*, and ρ_i^* parameters for solvents and PVAC are summarized in Table I. The solvent chemical potential is equal to:

$$\mu_{LF}/RT = \ln\varphi_1 + (1 - r_1/r_2) + r_1\tilde{\rho}X_{12} + r_1\left\{\frac{-\tilde{\rho}}{\tilde{T}_1} + \frac{\tilde{P}_1\tilde{v}}{\tilde{T}_1} + (\tilde{v} - 1)\ln(1 - \tilde{\rho}) + \frac{\ln\tilde{\rho}}{r_1}\right\} \tag{28}$$

Table I Lattice Fluid Equation of State Parameters (Sanchez and Panayiotou, 1994)

	T* (K)	P* (MPa)	ρ^* (kg/m^3)
Acetone	484	533	917
Methyl acetate	468	517	1094
Chloroform	512	456	1688
PVAC	590	509	1283

where parameter X_{12} is:

$$X_{12} = (\varepsilon_{11} + \varepsilon_{22} + 2\varepsilon_{12})/RT \tag{29}$$

The pure solvent chemical potential is given as follows:

$$\mu^0_{LF}/RT = r_1\left\{\frac{-\tilde{\rho}_1}{\tilde{T}_1} + \frac{\tilde{P}_1\tilde{v}_1}{\tilde{T}_1} + (\tilde{v}_1 - 1)\ln(1-\tilde{\rho}_1) + \frac{\ln\tilde{\rho}_1}{r_1}\right\} \tag{30}$$

The ζ parameter for the PVAC-acetone system was equal to unity, as shown by Luengo et al. (1994). Similarly, for the PVAC-methyl acetate system, ζ was found equal to 1.012 by comparing the Flory-Huggins chemical potential with the lattice fluid chemical potential Equations (28)–(30). Finally, the ζ parameter for the PVAC-chloroform system was found equal to 1.023 by fitting the activity coefficients as determined by sorption equilibrium experiments (Ju et al., 1981b). Introducing the effect of hydrogen bonding between chloroform and PVAC and applying lattice fluid with hydrogen bonding thermodynamics yields a ζ value closer to unity. A detailed presentation of the lattice fluid with hydrogen bonding theory is given by Panayiotou and Sanchez (1991).

The main advantage of lattice fluid thermodynamics over the Flory-Huggins theory is the introduction of an accurate equation of state describing variation of polymer density with constituents' concentration and temperature, including mixing phenomena (Sanchez and Lacombe, 1976a, 1976b). Additionally, this theory describes chemical potential variation with temperature and concentration more accurately than the Flory-Huggins theory. From a modeling point of view, lattice fluid theory is more attractive even in the case when there is a lack of experimental data for the density dependence on concentration and temperature.

The specific heat capacity and the thermal conductivity of the polymer solution were calculated from pure substance data by the following simple mixing rule:

$$P = P_1\omega_1 + P_2(1-\omega_1) \tag{31}$$

where P is property of the solution, ω_1 is weight fraction of the solvent, and P_1 and P_2 denote corresponding property of the solvent and PVAC, respectively.

The thermophysical properties of pure liquid solvents, PVAC, and glass support are given in standard references.

The Diffusion Coefficient of Solvent in PVAC. According to Crank (1975) the binary diffusion coefficient, D, is related in terms of self-diffusion

coefficient, D^*, and thermodynamic properties by the following expression:

$$D = \frac{D^* \rho_1}{RT}\left(\frac{\partial \Delta\mu_1}{\partial \rho_1}\right); \qquad \Delta\mu_1 = \mu_{\mathrm{LF}} - \mu^0_{\mathrm{LF}} \tag{32}$$

where ρ_1 and μ_1 are mass concentration and chemical potential of the solvent, respectively. From Equations (28)–(30) the derivative of solvent chemical potential with respect to the solvent mass concentration is directly calculated.

In the present work, we utilize the Vrentas and Duda (1977a, 1977b) equation for self-diffusion coefficient that includes concentration and temperature dependence of diffusion coefficient. According to the free volume diffusion model developed by Vrentas and Duda, solvent self-diffusion coefficient in a polymer solution, D^*, is given as follows:

$$D^* = D_0 \exp\left(\frac{-E}{RT}\right) \exp\left(\frac{-(\omega_1 V_1^* + (1-\omega_1)\xi V_2^*)}{\omega_1\left(\frac{K_{11}}{\gamma}\right)(K_{21} - T_{g1} + T) + (1-\omega_1)\left(\frac{K_{12}}{\gamma}\right)(K_{22} - T_{g2} + T)}\right) \tag{33}$$

Here, subscripts 1 and 2 refer to solvent and PVAC, respectively. D_0 is a pre-exponential factor, E is the critical energy that a molecule must possess to overcome the attractive forces holding to its neighbors, and γ is an overlap factor that is introduced because the same free volume is available to more than one molecule. V_i^* is specific hole free volume of the ith component required for a diffusion jump, and ξ represents the ratio of the critical molar volume of the jumping unit of solvent to that of polymer. K_{11} and K_{21} are free volume parameters for solvent while K_{12} and K_{22} are those for polymer. T_{gi} is glass transition temperature of ith component. The free volume parameters for solvents and PVAC are given in Table II.

Heat and Mass Transfer Coefficients. The heat transfer coefficient, h, is calculated by an empirical correlation (Perry and Green, 1984) for heat transfer under free convention conditions to a cooled, horizontal square plate, facing upward:

$$\frac{hw}{K^f} = 0.54(Gr\,\mathrm{Pr})^{0.25} \tag{34}$$

Table II Solvent and Polymer Free Volume Parameters (Hong, 1995)

A. Solvents	$V_1^* \times 10^3$ (m^3/kg)	$(k_{11}/\gamma) \times 10^6$ (m^3/kg K)	K_{21}-T_{g1} (K)	$D_0 \times 10^8$ (m^2/s)	E (J/gmol)
Acetone	0.943	1.86	− 53.33	3.6	0
Methyl acetate	0.855	1.25	− 38.5	5.23	0
Chloroform	0.51	0.71	− 29.43	4.07	0
B. Polymer	$V_2^* \times 10^3$ (m^3/kg)	$(k_{12}/\gamma) \times 10^7$ (m^3/kg K)	K_{22}-T_{g2} (K)		
PVAC	0.728	4.33	− 258.2		

The mass transfer coefficient, k_G, is calculated from the above correlation by invoking a heat and mass transfer analogy and using a correction term for high fluxes, obtained from film theory (Bird et al., 1960):

$$k_G = 0.54(\mathrm{Gr\ Sc})^{0.25}\left(\frac{c\ D^f}{w}\right)\frac{M_s}{P(x_s - x_g)}\ln\left(\frac{1 - x_g}{1 - x_s}\right) \tag{35}$$

where w is width of the plate, c is overall molar density, and M_s denotes molecular weight of solvent. K^f and D^f represent thermal conductivity of the gas phase and binary diffusion coefficient of solvent vapor in air, respectively. Superscript "f" represents properties evaluated at "mean gas phase temperature" $T_f = (T_s + T_g)/2$ and "mean solvent vapor mole fraction" $x_f = (x_s + x_g)/2$, with $T_g = T_0$.

Gr, Pr, and Sc represent Grashof, Prandtl, and Schmidt numbers of gas phase, respectively. These numbers have their standard definitions. Data for thermophysical properties of solvent vapor and air are available in standard references (Dean, 1973; VDI, 1974; Perry and Green, 1984). As shown by Verros and Malamataris (1999; 2001b), these correlations for heat and mass transfer accurately reproduce experimental results for temperature at the gas-liquid interface.

The solvent mole fraction at interface, x_s, can be written in terms of its chemical potential ($\Delta\mu_1/RT$) as:

$$x_s = e^{\Delta\mu_1/RT} P_1^{sat}/P \tag{36}$$

where P_1^{sat} is pure solvent vapor pressure calculated by an Antoine's equation (Dean, 1973).

Finite Element Formulation

The resulting system of governing equations (Equations (12)–(14)) augmented by the moving boundary equation (Equation (22)) along the initial and boundary conditions is solved with Galerkin finite elements. According to this method, the final formulation of weighted residuals (after expanding the unknown variables in quadratic basis functions, introducing convective terms in the governing equations due to the transformation of partial to total time derivatives and applying divergence theorem) becomes:

$$\mathrm{R}_{\mathrm{M}}^{\mathrm{i}} = \int_0^{\mathrm{s}} \left[\mathrm{C}_1 \frac{\mathrm{d}\omega_1}{\mathrm{d}\tau}\varphi^{\mathrm{i}} - \frac{\mathrm{d}\eta}{\mathrm{d}\tau}\mathrm{C}_1 \frac{\partial\omega_1}{\partial\eta}\varphi^{\mathrm{i}} + \frac{\partial\varphi^{\mathrm{i}}}{\partial\eta}\left(\mathrm{C}_1\mathrm{C}_2 \frac{\partial\omega_1}{\partial\eta}\right)\right] \mathrm{d}\eta - \mathrm{C}_1\mathrm{C}_2 \frac{\partial\omega_1}{\partial\eta}\varphi^{i}\Big|_{\eta=0}^{\eta=\mathrm{s}} \tag{37}$$

$$R_E^i = \int_0^s \left[C_3 \frac{d\Theta}{d\tau}\varphi^i - \frac{d\eta}{d\tau} C_3 \frac{\partial\Theta}{\partial\eta} + \frac{\partial\varphi^i}{\partial\eta}\left(C_4 \frac{\partial\Theta}{\partial\eta}\right)\right] d\eta - C_4 \frac{\partial\Theta}{\partial\eta}\varphi^i\Big|_{\eta=0}^{\eta=s} \tag{38}$$

$$R_E^i = \int_{-L_{\mathrm{sup}}/L_0}^{0} \left[\frac{\partial\Theta_{\mathrm{sup}}}{\partial\tau}\varphi^i + \frac{\partial\varphi^i}{\partial\eta}\left(C_5 \frac{\partial\Theta_{\mathrm{sup}}}{\partial\eta}\right)\right] d\eta - C_5 \frac{\partial\Theta_{\mathrm{sup}}}{\partial\eta}\varphi^i\Big|_{\eta=-L/L_{\mathrm{sup}}}^{\eta=0} \tag{39}$$

$$\mathrm{R}_{\mathrm{S}} = \rho_{\mathrm{s}}(1-\omega_1)\mathrm{d}s/\mathrm{d}\tau - C_6(x_s - x_g)V_1/V_2 \tag{40}$$

The computational domain is discretized in 15 finite elements. Residuals are evaluated numerically using three-point Gaussian integration, and time integration follows the Euler backward method. The resulting system of nonlinear algebraic equations is solved with Newton-Raphson iteration according to scheme $\mathbf{q}^{(\mathbf{n}+\mathbf{1})} = \mathbf{q} - \mathbf{J}^{-1}\mathbf{R}(\mathbf{q}^{(\mathbf{n})})$, where $\mathbf{q}$ is the vector of unknowns and $\mathbf{J}$ is the Jacobian matrix of residuals $\mathbf{R}$ with respect to the nodal unknowns $\mathbf{q}$. The maximum time step was equal to 10^{-2}. The computer program exhibits quadratic convergence in three to five iterations at each time step. Any additional mesh refinement or time step decrease has an improvement of less than 10^{-6} in the accuracy of the solution.

A detailed presentation of the finite element technique that enables simultaneous solution of the primary unknowns of the problem (solvent weight fraction and temperature) with the moving boundary can be found in Kistler and Scriven (1983) and Finlayson (1992).

RESULTS AND DISCUSSION

In order to estimate the diffusion coefficients, gravimetric data of solvent evaporation rate was compared with model predictions utilizing nonlinear regression analysis. The objective function requires the sum of squares of differences between the predicted and measured solvent evaporation rate to be minimal. The primary unknown in the parameter estimation procedure was ξ (see Equation (33)). If the resulting fitting between model predictions and experimental data was not satisfactory, quantities D_0 and E were added to the estimation procedure.

The resulting fitting for acetone evaporation is shown in Figures 2 and 3. The estimated value of ξ was 0.59 ± 0.02. This result is in complete agreement with the reported value (0.6) of Arnould and Laurence (1992) who measured diffusion coefficient of gaseous acetone in PVAC at the limit of pure polymer. Both experiment and model predictions show that as the initial polymer solution thickness increases, the rate of evaporation decreases since the solvent is provided at the surface with lower rate. Variation of temperature with time at the gas liquid interface is shown in Figure 4. Overall temperature variation is from 10 to 20°C, which is the range of validity of estimated diffusion coefficients.

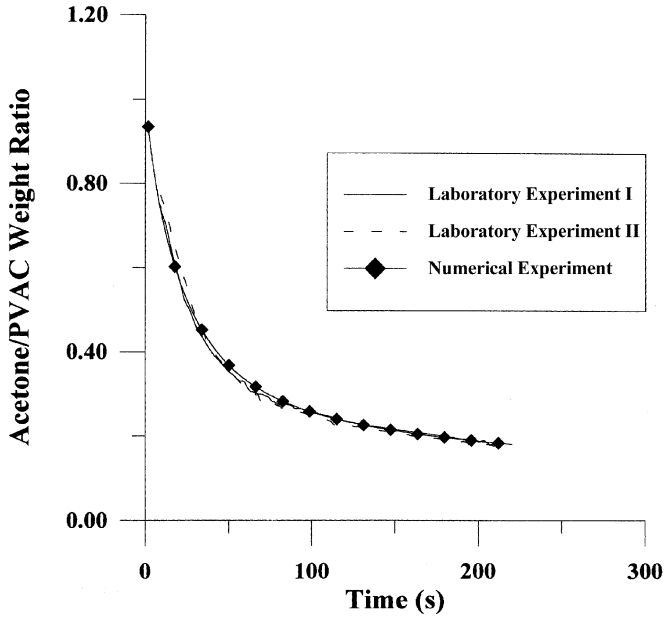

Figure 2. Comparison of model predictions for acetone evaporation rate with experimental data. $L_0 = 180\,\mu m$, $\omega_{10} = 0.5$, $T_0 = 20 \pm 1°C$.

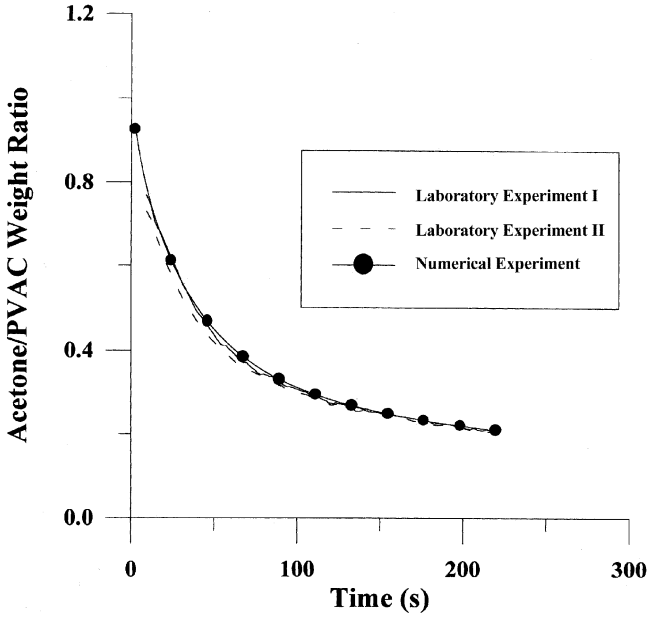

Figure 3. Comparison of model predictions for acetone evaporation rate with experimental data. $L_0 = 220\,\mu m$, $\omega_{10} = 0.5$, $T_0 = 20 \pm 1°C$.

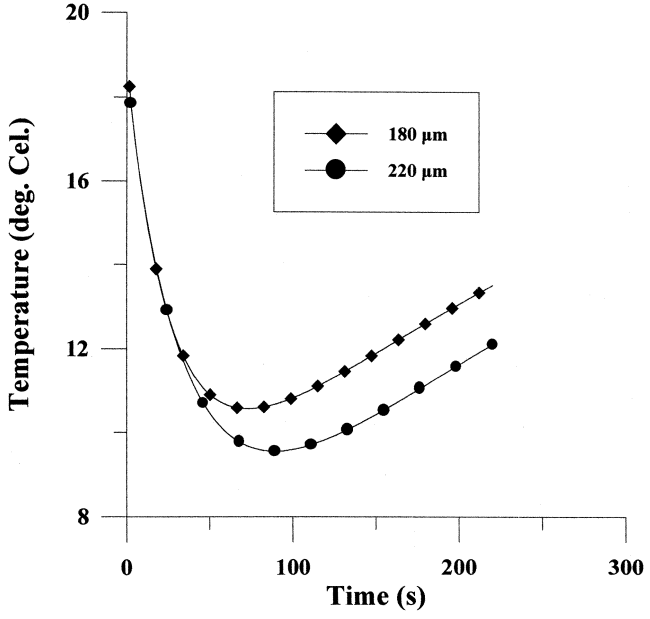

Figure 4. Model predictions for polymer solution surface temperature. Experimental conditions as in Figures 2 and 3.

The temperature minimum of the thinner solution (180 μm) is reached faster than for the thicker one (240 μm) as expected due to a higher evaporation rate. The minimum value of temperature of the thicker solution is smaller because the amount of evaporated solvent is larger. This behavior has also been observed in the binary system acetone-CA (Verros and Malamataris 1999, 2001a).

Figure 5 depicts the profiles of acetone weight fraction as a function of dimensionless thickness. Variation of acetone weight fraction was from 0.6 to almost zero, which is the rate of validity of estimated diffusion coefficients. In the beginning of the evaporation process, a smooth decrease in the acetone profile is observed. As evaporation proceeds, steep gradients are exhibited, and the value of acetone weight fraction at the interface is close to zero. This behavior is attributed to the fact that diffusion in the polymer film is very slow due to increased polymer concentration, while evaporation at the surface is high, leading, thus, to steep gradients near the gas-liquid interface. Establishment of these steep gradients (at approximately 64 s) leads to further deceleration of the evaporation rate, because both diffusion and solvent evaporation at the interface become minimal due to increased polymer concentration throughout the solution. This causes small variation of acetone weight fraction at longer times, since in the first 64 s, 65% of evaporated acetone

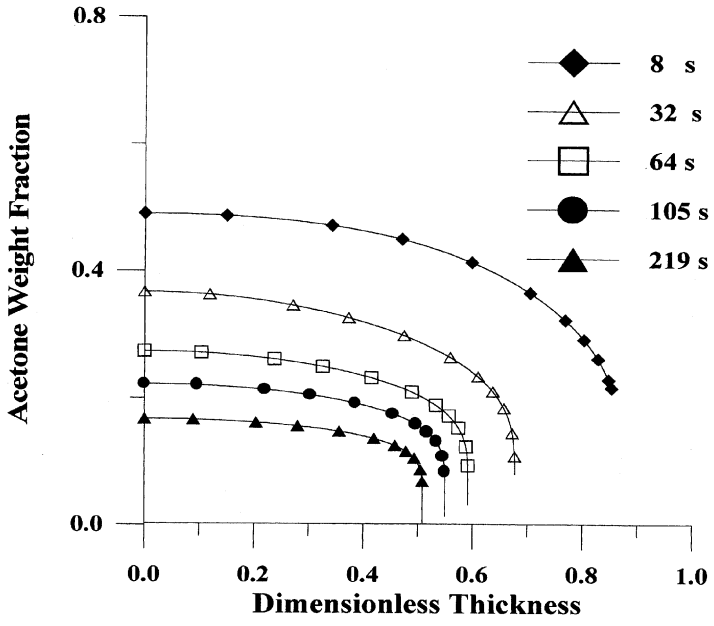

Figure 5. Acetone weight fraction profiles. $L_0 = 180\,\mu m$, $\omega_{10} = 0.5$, $T_0 = 20 \pm 1°C$.

is removed while the rest of the evaporated acetone is removed up to the end of the experiment at 220 s. This behavior is quite different from what is observed in the case of nonsolvent/solvent/polymer ternary solutions (Verros and Malamataris, 2001b), where steep gradients near the interface appeared from early evaporation times while solvent concentration at the bulk is almost unaffected.

Figures 6 and 7 show temperature profiles as a function of the solution thickness, prior to ($0 \leq t \leq 64$) and after minimum temperature attainment. Although the evaporation process is nonisothermal, the temperature in the polymer solution is uniform except for the beginning of the experiment where a small gradient is observed from the bottom up to the surface. This behavior is attributed to small variations of thermal conductivity and specific heat capacity with polymer concentration. Additionally, the heat transfer rates of the process are much higher than these of mass transfer as thermal diffusivity is of the order of $10^{-7}m^2/s$, compared to diffusion coefficient, which is of the order of $10^{-9}-10^{-17}m^2/s$ (Figure 8).

However, in Figure 6, temperature profiles have a slight negative slope as expected by the decrease in surface temperature due to acetone

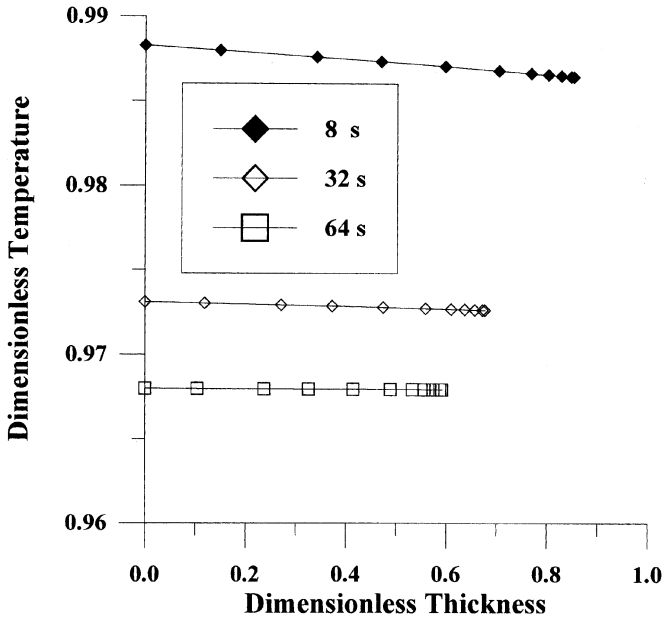

Figure 6. Temperature profiles prior to the minimum temperature attainment. $L_0 = 180\,\mu m$, $\omega_{10} = 0.5$, $T_0 = 20 \pm 1°C$.

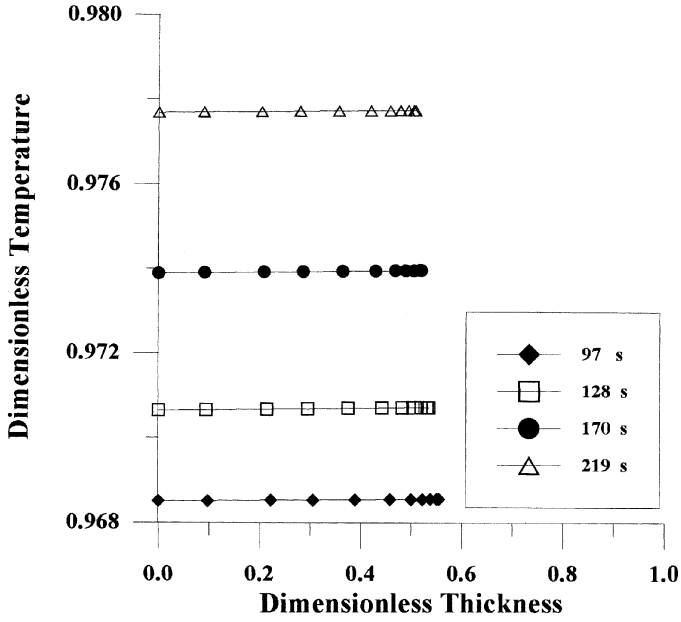

Figure 7. Temperature profiles after the minimum temperature attainment. $L_0 = 180$ μm, $\omega_{10} = 0.5$, $T_0 = 20 \pm 1°C$.

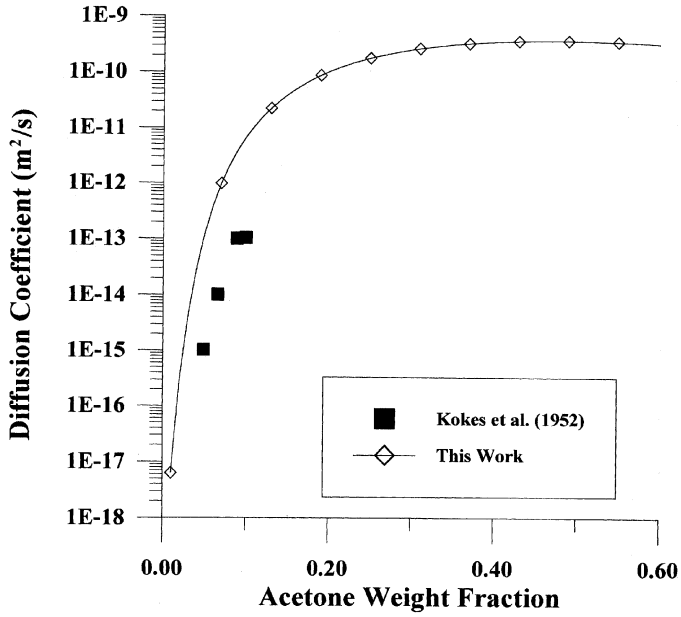

Figure 8. Acetone-PVAC binary diffusion coefficient at 20°C.

evaporation, while in Figure 7 slopes become positive because of the increase at surface temperature (see Figure 4).

In Figure 8, a comparison is made between estimated diffusion coefficients and measurements by Kokes et al. (1952). The estimated binary diffusion coefficient is almost one order of magnitude above the measured ones by acetone vapor sorption, and this difference is increased as acetone concentration increases. Similar differences between diffusion coefficients measured by sorption and estimated by solvent evaporation for the system cellulose acetate-water were reported by Verros and Malamataris (2001b). This discrepancy is attributed to inherent differences between sorption experiments and the liquid evaporation method.

In Figures 9 and 10, an excellent agreement is depicted between model predictions for methyl acetate evaporation rate and experimental data for estimated values of ξ in the range 0.59 ± 0.05. The corresponding value for ξ reported by Arnould and Laurence (1992) is 0.65. During the experiments the temperature varied from 20°C to 10°C as shown in Figure 11. Comparing Figure 11 and Figure 4 we observe that the minimum temperature for the methyl acetate-PVAC system is the same in both experiments, while the minimum temperature for the acetone-PVAC system is attained at the same time for both experiments.

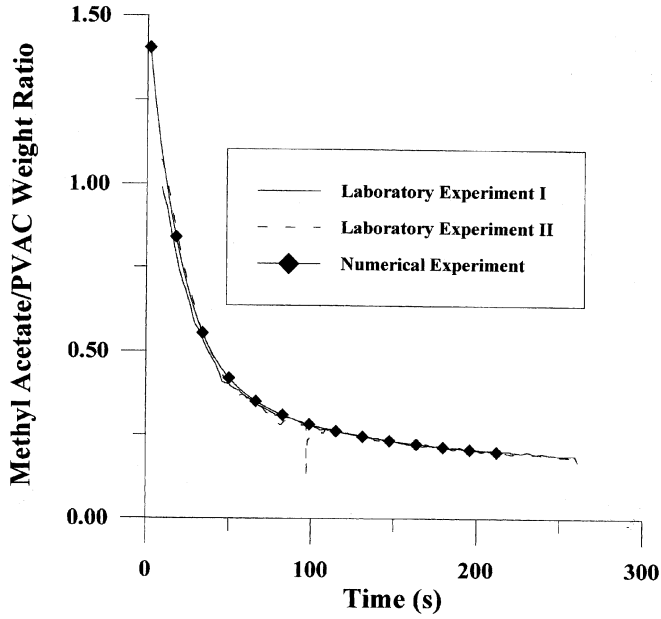

Figure 9. Comparison of model predictions for methyl acetate evaporation rate with experimental data. $L_0 = 180\,\mu m$, $\omega_{10} = 0.6$, $T_0 = 20 \pm 1°C$.

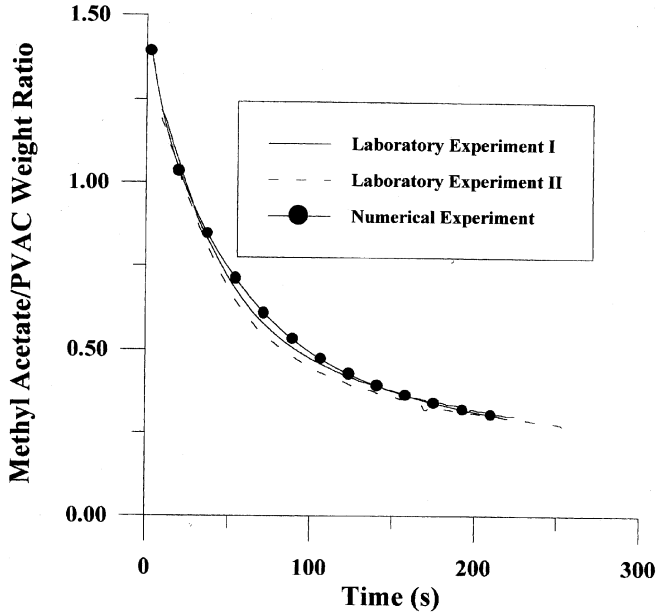

Figure 10. Comparison of model predictions for methyl acetate evaporation rate with experimental data. $L_0 = 240\,\mu m$, $\omega_{10} = 0.6$, $T_0 = 20 \pm 1°C$.

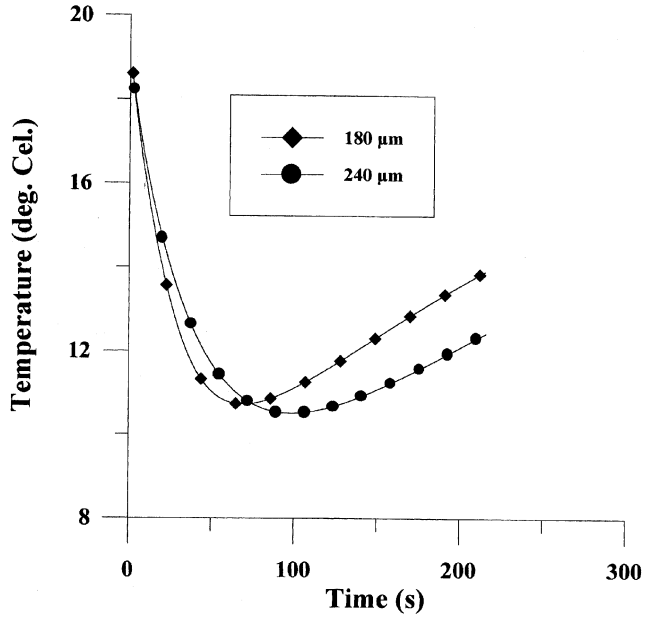

Figure 11. Model predictions for polymer solution surface temperature. Experimental conditions as in Figures 9 and 10.

The excellent agreement between model prediction and experimental data for the chloroform evaporation rate is illustrated in Figure 12. The estimated values for D_0, E, and ξ were 2.82 m^2/s, 42800 J/gmol, and 0.69, respectively. Corresponding values for D_0, E, and ξ, reported by Ju et al. (1981b; 1992b) are 6.12 10^{-4} m^2/s, 30222 J/gmol, and 0.64, respectively. They applied Vrentas-Duda free volume theory to correlate binary diffusion coefficients obtained from sorption experiments. In Figure 13, predicted binary diffusion coefficients are compared with experimental data of Ju et al. (1981b). The observed discrepancy is attributed to the different range of temperature and to inherent differences between the solvent evaporation method and sorption experiments. In Figure 14, it is shown how temperature at the gas-liquid interface varies during evaporation. Upper and lower limits, for temperature are 20°C and 15°C, respectively.

Figure 15 depicts the chloroform profiles along the solution as function of time. Compared to the case of acetone (Figure 5), more solvent (chloroform) is trapped in the solution. This phenomenon is attributed to lower values of diffusion coefficients (Figure 13), which is caused by high critical energy (E) of diffusion and difference in chemical affinity.

Finally, errors introduced by uncertainty of values of heat and mass transfer coefficients are negligible since the evaporation process is controlled by diffusion in the liquid phase. More specifically, it was shown

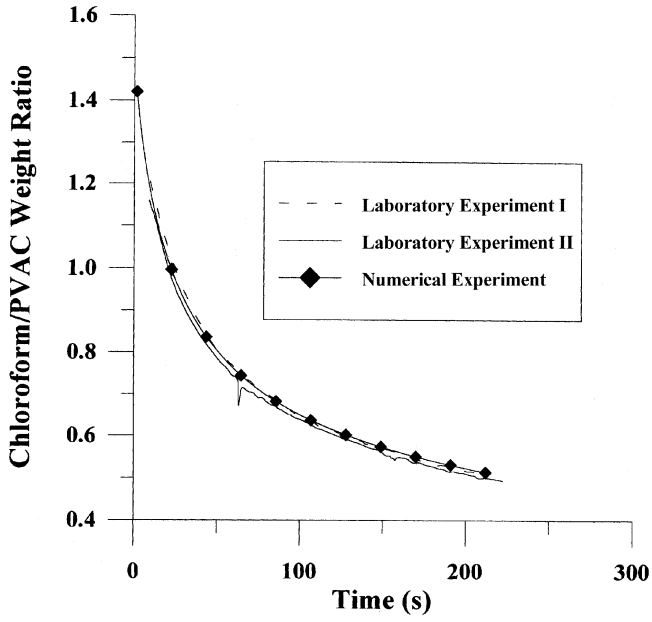

Figure 12. Comparison of model predictions for chloroform evaporation rate with experimental data. $L_0 = 180\,\mu m$, $\omega_{10} = 0.6$, $T_0 = 20 \pm 1°C$.

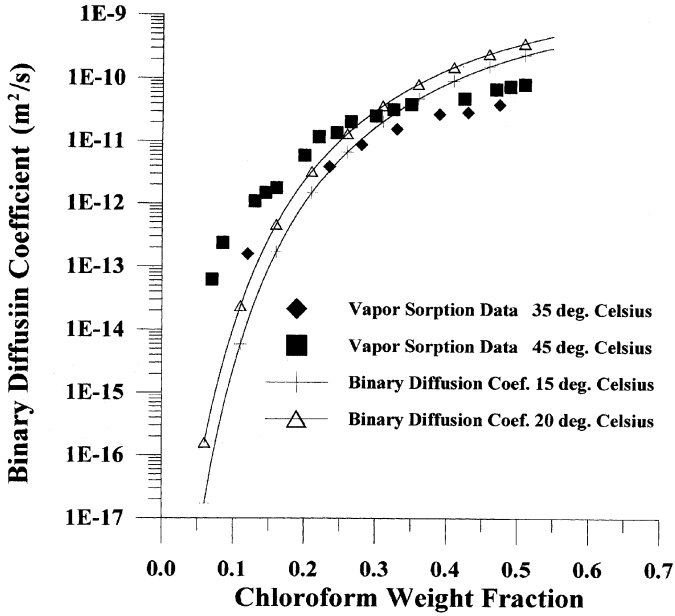

Figure 13. Chloroform-PVAC binary diffusion coefficient.

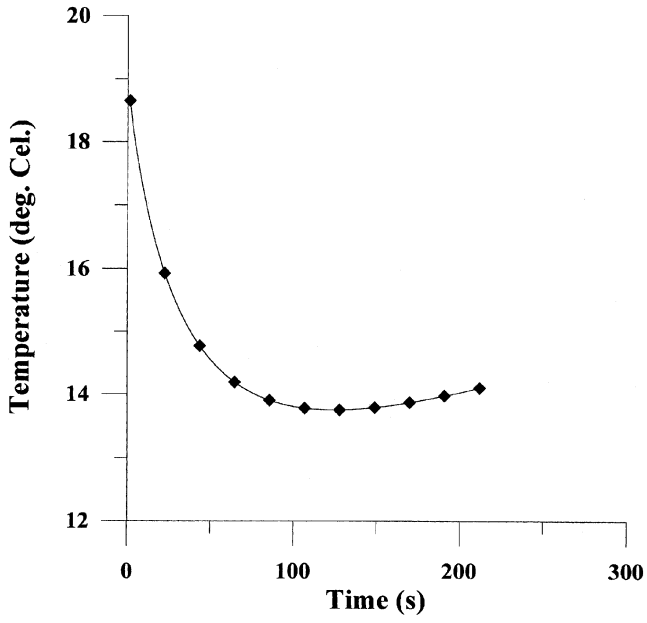

Figure 14. Model predictions for polymer solution surface temperature. Experimental conditions as in Figure 12.

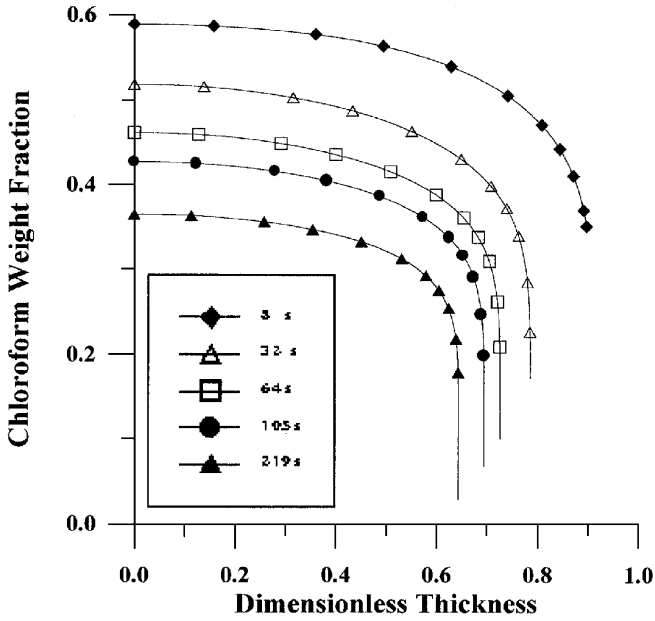

Figure 15. Chloroform weight fraction profiles. $L_0 = 180\,\mu m$, $\omega_{10} = 0.6$, $T_0 = 20 \pm 1°C$.

(Verros and Malamataris, 1999) that variation of heat and mass transfer coefficients by $\pm 100\%$ does not affect evaporation rate.

CONCLUSIONS

For the first time, in this work we estimated diffusion coefficients of three solvents, namely, acetone, methyl acetate, and chloroform in amorphous PVAC, using the solvent evaporation method. The experimentally determined evaporation rate from polymer-solvent thin films was compared with model predictions in order to estimate diffusion coefficients based on free volume theory. For this purpose, the coupled heat and mass transfer of the evaporation process is modeled as a one-dimensional numerical experiment with a moving boundary. Lattice fluid thermodynamics was used to describe variations of polymer solution density and solvent chemical potential with concentration and temperature. The resulting complex system of governing equations along with appropriate initial and boundary conditions is solved with Galerkin finite elements. The estimated unknown parameters of diffusion coefficient correlations, based on free-volume theory, are in satisfactory agreement with available experimental data from the literature.

Discrepancies between the estimated diffusion coefficients and experimental data are due to the complexity in obtaining accurate measurements and to uncertainty of model parameters. Comparing the diffusion behavior of three solvents, we observed that acetone and methyl acetate are trapped in PVAC in smaller amounts than chloroform. This is attributed to the high critical energy of chloroform diffusion. In all cases, the nonisothermal character of the diffusion process has been confirmed, although the temperature at each time step was almost uniform in the solution. Steep gradients in the solvent concentration were observed from the beginning of the evaporation and gradually become steeper at the end of the process. It is believed that the present work establishes the solvent evaporation technique as a general tool that may be applied to other polymer-solvent systems for the estimation of diffusion coefficients over a wide range of concentration and temperature, providing a valuable insight into the physics of diffusion and a more rational design of polymeric products.

ACKNOWLEDGMENT

G. D. V. is thankful to Prof. C. Panayiotou, Chemical Engineering Department, Aristotle University of Thessaloniki, for his kind support.

NOMENCLATURE

C_p	specific heat capacity of the polymer solution, J/kg.K
D	binary diffusion coefficient, m^2/s
h	heat transfer coefficient, W/m^2K
k	thermal conductivity of the polymer solution, W/mK
P	total pressure, Pa
t	time, s
T	temperature, K
x_s	solvent mole fraction at the liquid layer-gas phase interface
x_g	solvent mole fraction far away from the interface

Greek letters

ΔH	solvent latent heat of vaporization, J/kg
ε	emissivity of the polymer solution
ρ_1	solvent mass concentration, kg/m^3
ρ_s	density of the polymer solution, kg/m^3
σ	Stefan-Boltzmann constant, W/m^2K^4

Subscript

sup	properties and variables of the support

REFERENCES

Alsoy, S. and Duda, J. L. (1999). Modeling of multicomponent drying of polymer films, *AIChE J*. **45**(4), 896.

Anderson, J. E. and Ullman, R. (1973). Mathematical analysis of factors influencing the skin thickness of asymmetric reverse osmosis membranes, *J. Appl. Phys*. **44**, 4303.

Arnould, D. and Laurence, J. L. (1992). Size effects on solvent diffusion in polymers, *Ind. Eng. Chem. Res*. **31**, 218.

Ataka, M. and Sasaki, K. (1982). Gravimetric analysis of membrane casting. I: cellulose acetate-acetone binary casting solutions, *J. Membrane Sci*. **11**, 11.

Bird, R. B., Stewart, R., and Lightfoot, E. N. (1960). *Transport Phenomena*, John Wiley, New York.

Cairncross, R. A., Jeyadef, E. N., Dunham, R. F., Evans, K. L., Francis, F., and Scriven, L. E. (1995). Modeling and design of an industrial dryer with convective and radiant heating, *J. Appl. Polym. Sci*. **58**, 1279.

Crank, J. (1975). *The Mathematics of Diffusion*, Clarendon Press, Oxford.

Crank, J. and Park, G. S. (1968). Methods of measurement, In: *Diffusion in Polymers*, J. Crank and G. S. Park, eds., Academic Press, New York.

Cussler, E. L. (1984). *Diffusion Mass Transfer in Fluid Systems*, Cambridge University Press, Cambridge.

Dean, J. A. (1973). *Lange's Handbook of Chemistry*, 11th ed., McGraw-Hill, New York.

Finlayson, B. A. (1992). *Numerical Methods for Problems with Moving Fronts*, Ravenna Park Publishing, Seattle.

Guerrier, B., Bouchard, C., Allain, C., and Benard, C. (1998). Drying kinetics of polymer films, *AIChE J*. **44**(4), 791.

Hong, S. (1995). Prediction of polymer/solvent solution behavior using free-volume theory, *Ind. Eng. Chem. Res*. **34**, 2536.

Ju, S. T., Duda, J. L., and Vrentas, J. S. (1981a). Influence of temperature on the diffusion of solvents in polymers above the glass transition temperature, *Ind. Eng. Chem. Prod. Res. Dev*. **20**, 330.

Ju, S. T., Liu, H. T., Duda, J. L., and Vrentas, J. S. (1981b). Solvent diffusion in amorphous polymers, *J. Appl. Polym. Sci*. **26**, 3735.

Kistler, S. F. and Scriven, L. E. (1983). Coating Flows, In: *Computational Analysis of Polymer Processing*, J. R. A. Pearson and S. M. Richardson, eds., Applied Science Publishing, London.

Kokes, R. J., Long, F. A., and Hoard, J. L. (1952). Diffusion of acetone into polyvinyl acetate above and below the second-order transition, *J. Chem. Phys*. **20**, 1711.

Luengo, L., Rabio, R. G., Sanchez, I. C., and Panayiotou, C. G. (1994). The system poly(4-hydroxystyrene)/poly(vinyl acetate)/acetone: an experimental and theoretical study, *Makromol. Chem. Phys*. **195**, 1043.

Panayiotou, C. G. and Sanchez, I. C. (1991). Hydrogen bonding in fluids: an equation-of-state approach, *J. Phys. Chem.* **95**, 10090.

Park, G. S. (1961). Radioactive studies of diffusion in polymer systems. Part 3: sorption and self-diffusion in the acetone + cellulose acetate system, *Trans. Faraday Soc.* **57**, 2314.

Perry, R. H. and Green, D. (1984). *Perry's Chemical Engineers' Handbook*, 6th ed., McGraw-Hill, New York.

Price, Jr., P. E., Wang, S., and Romdhane, I. H. (1997). Extracting effective diffusion parameters from drying experiments, *AIChE J.* **43**, 1925.

Reuvers, A. J. and Smolders, C. A. (1987). Formation of membranes by means of immersion precipitation. Part II: the mechanism of formation of membranes prepared from the system cellulose acetate-acetone-water, *J. Membrane Sci.* **34**, 67.

Sanchez, I. C. and Lacombe, R. H. (1976a). An elementary molecular theory of classical fluids: pure fluids, *J. Phys. Chem.* **80**, 2352.

Sanchez, I. C. and Lacombe, R. H. (1976b). Statistical thermodynamics of fluid mixtures, *J. Phys. Chem.* **80**, 2568.

Sanchez, I. C. and Panayiotou, C. G. (1994). Equation of state thermodynamics of polymer and related solutions, In: *Models for Thermodynamic and Phase Equilibrium Calculations*, S. I. Sandler, ed., Marcel Dekker, New York.

Sanopoulou, M., Roussis, P. P., and Petropoulos, J. H. (1995). A detailed study of the viscoelastic nature of vapor sorption and transport in a cellulosic polymer. I: origin and physical implications of deviations from Fickian sorption kinetics, *J. Polym. Sci. Part B: Polym. Phys.* **33**, 993.

Shojaie, S. S., Krantz, W. B., and Greenberg, A. R. (1992). Development and validation of a model for the formation of evaporatively cast polymeric films. *J. Mat. Proc. Man. Sci.* **1**, 181.

Tyrrell, H. J. V. and Harris, K. R. (1984). *Diffusion in Liquids: A Theoretical and Experimental Study*, Butterworths, London.

VDI-Verein Deutscher Ingenieure. (1974). *VDI-Warmeatlas*, VDI-Verlag, Dusseldorf.

Verros, G. D. and Malamataris, N. A. (1999). Estimation of diffusion coefficients in acetone-cellulose acetate solutions, *Ind. Eng. Chem. Res.* **38**, 3572.

Verros, G. D. and Malamataris, N. A. (2001a). Finite element analysis of polymeric membrane and coating formation by solvent evaporation, *Comput. Mech.* **27**, 332.

Verros, G. D. and Malamataris, N. A. (2001b). Computer aided estimation of diffusion coefficients in polymer/non-solvent systems, *Macromol. Theory Simul.* **10**, 737.

Vrentas, J. S. and Duda, J. L. (1977a). Diffusion in polymer-solvent systems. I: re-examination of the free-volume theory, *J. Polym. Sci. Part B: Polym. Phys.* **15**, 403.

Vrentas, J. S. and Duda, J. L. (1977b). Diffusion in polymer-solvent systems. II: a predictive theory for the dependence of diffusion coefficients on temperature,

concentration and molecular weight, *J. Polym. Sci. Part B: Polym. Phys.* **15**, 417.

Vrentas, J. S. and Vrentas, C. M. (1994). Drying of solvent-coated polymer films, *J. Polym. Sci. Part B: Polym. Phys.* **32**, 187.

Vrentas, J. S., Vrentas, C. M., and Faridi, N. (1996). Effect of solvent size on solvent self-diffusion in polymer-solvent systems, *Macromolecules* **29**, 3272.

Zielinski, J. M. and Duda, J. L. (1992). Predicting polymer/solvent diffusion coefficients using free volume theory, *AIChE J.* **38**, 405.

Zielinski, J. M. and Duda, J. L. (1996). Solvent diffusion in polymeric systems, In: *Polymer Devolatilization*, R. J. Albalak, ed., Marcel Dekker, New York.